



# Low-loss and low-crosstalk multimode waveguide bend on silicon

XIAOHUI JIANG, HAO WU, AND DAOXIN DAI\*

*Centre for Optical and Electromagnetic Research, State Key Laboratory for Modern Optical Instrumentation, Zhejiang Provincial Key Laboratory for Sensing Technologies, Zhejiang University, Zijingang Campus, Hangzhou 310058, China*

\*[dxdai@zju.edu.cn](mailto:dxdai@zju.edu.cn)

**Abstract:** A low-loss and low-crosstalk multimode waveguide bend is proposed and demonstrated for mode-division-multiplexed optical interconnects. The proposed 90°-bend is composed of two identical 45°-bends, which are defined as modified Euler curves. For the designed 90° Euler-bend with a core width of 2.36  $\mu\text{m}$  for supporting four TM-polarization modes, it is allowed to achieve an effective radius as small as 45  $\mu\text{m}$ , which is about 1/4 of the radius ( $\sim 175 \mu\text{m}$ ) for a regular 90° arc-bend. In theory, this proposed 90° Euler-bend has very low excess losses ( $<0.1 \text{ dB}$ ) and very low inter-mode crosstalks ( $<-25 \text{ dB}$ ) over a broad wavelength-band. A silicon photonic integrated circuit is designed, fabricated and characterized by integrating a pair of mode (de)multiplexers and a multimode bus waveguide with a Euler S-bend consisting of two cascaded 90° Euler-bends. The measurement results show that the fabricated Euler S-bend has low excess losses of  $<0.5 \text{ dB}$  and low inter-mode crosstalks of  $<-20 \text{ dB}$  over a broad band from 1520 nm to 1610 nm for all the 4 mode-channels of TM polarization.

© 2018 Optical Society of America under the terms of the [OSA Open Access Publishing Agreement](#)

## References and links

1. T. Mizuno and Y. Miyamoto, "High-capacity dense space division multiplexing transmission," *Opt. Fiber Technol.* **35**, 108–117 (2017).
2. D. X. Dai, "Silicon nanophotonic integrated devices for on-chip multiplexing and switching," *J. Lightwave Technol.* **35**(4), 572–587 (2017).
3. D. J. Richardson, J. M. Fini, and L. E. Nelson, "Space-division multiplexing in optical fibres," *Nat. Photonics* **7**(5), 354–362 (2013).
4. G. Li, N. Bai, N. Zhao, and C. Xia, "Space-division multiplexing: the next frontier in optical communication," *Adv. Opt. Photonics* **6**(4), 413–487 (2014).
5. D. Dai and J. E. Bowers, "Silicon-based on-chip multiplexing technologies and devices for Peta-bit optical interconnects," *Nanophotonics* **3**(4–5), 283–311 (2014).
6. H. D. Chen, Z. Zhang, B. J. Huang, L. H. Mao, and Z. Y. Zhang, "Progress in complementary metal-oxide-semiconductor silicon photonics and optoelectronic integrated circuits," *J. Semicond.* **36**(12), 121001 (2015).
7. Y. Vlasov and S. McNab, "Losses in single-mode silicon-on-insulator strip waveguides and bends," *Opt. Express* **12**(8), 1622–1631 (2004).
8. W. Bogaerts, P. Dumon, D. Van Thourhout, and R. Baets, "Low-loss, low-cross-talk crossings for silicon-on-insulator nanophotonic waveguides," *Opt. Lett.* **32**(19), 2801–2803 (2007).
9. D. Dai, Y. Shi, and S. He, "Comparative study of the integration density for passive linear planar light-wave circuits based on three different kinds of nanophotonic waveguide," *Appl. Opt.* **46**(7), 1126–1131 (2007).
10. Y. Y. Chen, J. Z. Yu, Q. F. Yan, and S. W. Chen, "Analysis on Influencing Factors of Bend Loss of Silicon-on-Insulator Waveguides," *J. Semicond.* **26**(13), 216 (2005).
11. L. H. Gabrielli, D. Liu, S. G. Johnson, and M. Lipson, "On-chip transformation optics for multimode waveguide bends," *Nat. Commun.* **3**(1), 1217 (2012).
12. D. X. Dai, J. Wang, and S. L. He, "Silicon multimode photonic integrated devices for on-chip mode-division-multiplexed optical interconnects," *Prog. Electromagnetics Res.* **143**, 773–819 (2013).
13. D. Dai, "Multimode optical waveguide enabling microbends with low inter-mode crosstalk for mode-multiplexed optical interconnects," *Opt. Express* **22**(22), 27524–27534 (2014).
14. C. Sun, Y. Yu, G. Chen, and X. Zhang, "Ultra-compact bent multimode silicon waveguide with ultralow inter-mode crosstalk," *Opt. Lett.* **42**(15), 3004–3007 (2017).
15. H. Xu and Y. Shi, "Ultra sharp multimode waveguide bending assisted with metamaterial based mode converters," *Laser Photonics Rev.* **12**(3), 1700240 (2018).
16. T. Chen, H. Lee, J. Li, and K. J. Vahala, "A general design algorithm for low optical loss adiabatic connections in waveguides," *Opt. Express* **20**(20), 22819–22829 (2012).

17. H. Lee, T. Chen, J. Li, O. Painter, and K. J. Vahala, "Ultra-low-loss optical delay line on a silicon chip," *Nat. Commun.* **3**(1), 867 (2012).
18. W. Bogaerts and S. K. Selvaraja, "Compact single-mode silicon hybrid rib/strip waveguide with adiabatic bends," *IEEE Photonics J.* **3**(3), 422–432 (2011).
19. D. J. Goodwill and J. Jiang, "Apparatus and method for a waveguide polarizer comprising a series of bends," U.S. patent 9690045 B2 (June 27, 2017).
20. X. Tu, M. Li, J. Jiang, D. Goodwill, P. Dumais, E. Bernier, H. Fu, and D. Geng, "Compact low-loss adiabatic bends in silicon shallow etched waveguides," in *Proceedings of IEEE International Conference on Group IV Photonics* (IEEE, 2016), pp. 48–49.
21. T. Fujisawa, S. Makino, T. Sato, and K. Saitoh, "Low-loss, compact, and fabrication-tolerant Si-wire 90° waveguide bend using clothoid and normal curves for large scale photonic integrated circuits," *Opt. Express* **25**(8), 9150–9159 (2017).
22. M. Cherchi, S. Ylinen, M. Harjanne, M. Kapulainen, and T. Aalto, "Dramatic size reduction of waveguide bends on a micron-scale silicon photonic platform," *Opt. Express* **21**(15), 17814–17823 (2013).
23. B. A. Dorin and W. N. Ye, "Two-mode division multiplexing in a silicon-on-insulator ring resonator," *Opt. Express* **22**(4), 4547–4558 (2014).
24. X. Wu, W. Zhou, D. Huang, Z. Zhang, Y. Wang, J. Bowers, and H. K. Tsang, "Low Crosstalk Bent Multimode Waveguide for On-chip Mode-Division Multiplexing Interconnects," in *Conference on Lasers and Electro-Optics*, OSA Technical Digest (online) (Optical Society of America, 2018), paper JW2A.66.
25. D. Dai, J. Wang, and Y. Shi, "Silicon mode (de)multiplexer enabling high capacity photonic networks-on-chip with a single-wavelength-carrier light," *Opt. Lett.* **38**(9), 1422–1424 (2013).

## 1. Introduction

The demand for high capacity optical interconnects grows rapidly in the past decades, and thus various advanced multiplexing technologies [1–4], including wavelength-division-multiplexing (WDM), polarization-division-multiplexing (PDM), spatial-division-multiplexing (SDM), and mode-division-multiplexing (MDM), have been developed. Among them, the MDM technology significantly increases the link capacity for a single wavelength carrier by transmitting multiple mode-channels in parallel along a multimode bus waveguide [4, 5]. It is well known that compact multimode waveguide bends are indispensable for routing the data transmission as well as designing photonic integrated circuits (PICs) flexibly. The compatibility with conventional electronic CMOS foundries makes silicon photonics popular an emerging competitive solution for next-generation scalable data communications [6]. As it is well known, the ultra-high index-contrast of silicon-on-insulator (SOI) strip waveguides enables an ultra-sharp bend with a radius as small as several microns when operating with the singlemode condition [7–10]. However, for multimode waveguide bends, the mode fields become asymmetric increasingly when the bending radius decreases [11–15]. For those multiple mode-channels propagating along the multimode bus waveguide with sharp bends, the mismatching between the modal fields in multimode straight waveguides (SWGs) and multimode bent waveguides (BWGs) introduces significant excess losses and inter-mode crosstalks [11–15].

Great efforts had been made to achieve compact multimode waveguide bends with low losses and low crosstalks [11–15]. In [11], Lucas et al. applied the transformation optics theory to diminish the mode mismatch by gradually varying the core-height of the BWG. For this case, some special fabrication processes are required, e.g., the grayscale lithography. A kind of vertical multimode waveguide supporting multiple modes in vertical direction was proposed to achieve a sharp bend (e.g.,  $\sim 5 \mu\text{m}$ ) enabling low losses and low crosstalks [13]. However, this does not work for the case when the top-silicon layer is thin, e.g., 220 nm, which has been used very popularly. In [14], a step-tapered mode converter was demonstrated to realize a compact waveguide bend with effective radius  $R = 10 \mu\text{m}$  (including the length of the mode converters) for two lowest-order modes. However, it is not easy to be extended for the multimode waveguide bends with more than two higher-order modes. Another novel mode converter with subwavelength-structured PMMA upper-cladding was introduced to enable a compact multimode waveguide bend with an effective radius  $R' = 45.8 \mu\text{m}$  for four TM mode-channels [15].

One might notice that the trajectory design method has been applied to realize adiabatic and low-loss waveguides for singlemode bus waveguides [16–21]. An algorithm for designing low-loss adiabatic connections in singlemode waveguides was proposed theoretically [16] and was demonstrated experimentally [17]. Various structures utilizing specific trajectories, such as polynomial spline [18], sine-circle-sine curve [19,20], Euler curve [21,22] have been used to realize the compact singlemode waveguides. In particular, for multimode waveguide bends, Bezier curve is applied to minimize mode mismatch at the SWG-BWG junction [23,24]. In this case, Bezier curve is designed by adjusting the form factor  $B$ . One usually prefers a small value for the form factor  $B$  in order to achieve a sufficiently large curvature radius at the SWG-BWG junction. On the other hand, a small value of  $B$  leads to a small curvature radius near the knee of the bend. As a result, the trajectory might not be adiabatic sufficiently, which makes the design inflexible. As it is well known, Euler curve has a variant curvature, which linearly increases from zero along the curve [21,22]. In this case, the modal fields in SWGs gradually convert to the modal fields in BWGs with low losses. However, the previous works focus on the design of singlemode waveguide bends [21,22]. One should notice that the situation becomes very complex for multimode waveguide bends due to the inter-mode crosstalk. In this paper, we propose and realize a low-loss and low-crosstalk multimode waveguide bend defined with a modified Euler curve. As an example, a  $90^\circ$  Euler-bend with a core width of  $2.36 \mu\text{m}$  for supporting four TM-polarization modes is realized with an effective radius as small as  $45 \mu\text{m}$ , which is about  $1/16$  of the size for a regular  $90^\circ$  arc-bend.

## 2. Structure and design

Figure 1(a) shows the schematic configuration of the present  $90^\circ$  Euler-bend composed of a pair of  $45^\circ$  modified-Euler bends, which is determined by the maximal and minimal curvature radii ( $R_{\max}$  and  $R_{\min}$ ). Correspondingly, the effective radius  $R_{\text{eff}}$  is defined as the radius of a  $90^\circ$  arc-bend in the square area occupied by the  $90^\circ$  Euler-bend, as shown in Fig. 1(b). The curvature of the modified Euler curve is defined as

$$\frac{d\theta}{dL} = \frac{1}{R} = \frac{L}{A^2} + \frac{1}{R_{\max}}, \quad (1)$$

where  $L$  is the curve length from the starting point  $(0, 0)$  to position  $(x, y)$ ,  $R$  is the curvature radius,  $A$  is a constant. The constant  $A$  is given by

$$A = \left[ L_0 / (1/R_{\min} - 1/R_{\max}) \right]^{1/2}, \quad (2)$$

where  $L_0$  is the curve length corresponding to the end-position  $(x_E, y_E)$  where  $R = R_{\min}$ . It can be transformed to be with the Cartesian coordinate system, as shown in Eqs. (3)-(4),

$$x = A \int_0^{L/A} \sin \left( \frac{\theta^2}{2} + \frac{A\theta}{R_{\max}} \right) d\theta, \quad (3)$$

$$y = A \int_0^{L/A} \cos \left( \frac{\theta^2}{2} + \frac{A\theta}{R_{\max}} \right) d\theta. \quad (4)$$

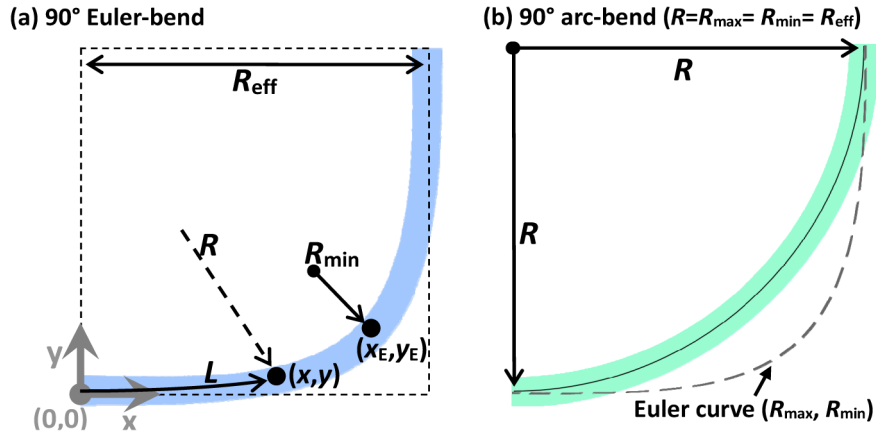


Fig. 1. Schematic configurations for 90°-bends. (a) The 90° Euler-bend composed of a pair of 45° modified Euler-curves with a maximum curvature radius  $R_{\max}$  at the starting point  $(0, 0)$  and a minimum curvature radius  $R_{\min}$  at the end point  $(x_E, y_E)$ ; (b) A regular 90° arc-bend with a constant radius  $R = R_{\text{eff}}$  (here the modified Euler curve is also shown by the dashed curve to give a comparison).

In order to minimize the excess losses and the inter-mode crosstalk, the design rule for choosing the bending radii  $R_{\max}$  and  $R_{\min}$  of the modified Euler bend is described as follows. (1) The maximal curvature radius  $R_{\max}$  should be large enough to void significant mode mismatch at the SWG-BWG junction; (2) The minimum curvature radius  $R_{\min}$  should as small as possible to be compact. Meanwhile, it should also be large enough to make the waveguide bended adiabatically. As an example, in this paper we consider the silicon-on-insulator (SOI) platform with a 220 nm top-silicon layer (i.e.,  $h_{\text{co}} = 220$  nm) and 2  $\mu\text{m}$   $\text{SiO}_2$  buried layer. The width of the multimode waveguide is chosen as 2.36  $\mu\text{m}$  for supporting four mode-channels of TM polarization when operating at the wavelength around  $\lambda_0 = 1550$  nm. Here we consider TM-polarization modes as an example because the high-performance mode (de)multiplexer for TM polarization is available in our lab.

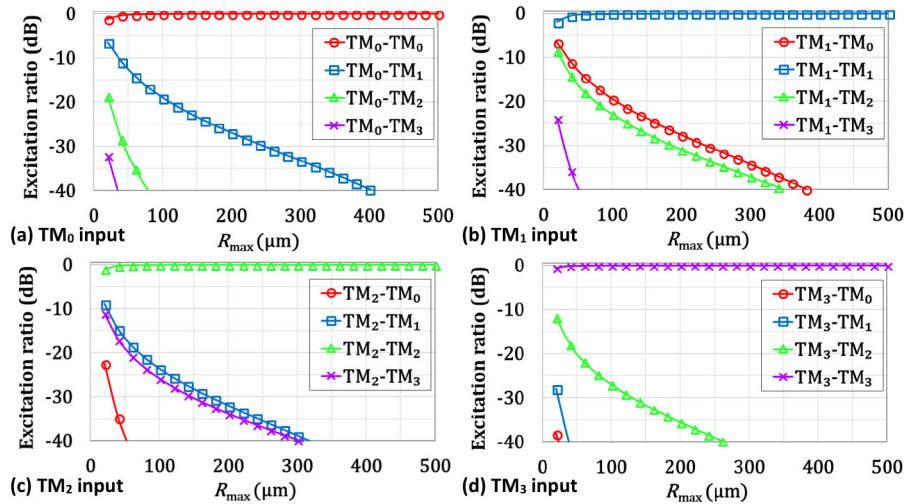


Fig. 2. Calculated mode excitation ratio  $\xi_{ji}$  from the  $i$ -th mode launched at the input SWG to the  $j$ -th mode in a BWG with a constant curvature radius  $R_{\max}$  varies for the cases with  $i = 0$  (a), 1 (b), 2 (c), and 3 (d), respectively.

In order to determine the maximal curvature radius  $R_{\max}$  for the modified Euler-bend, the mode mismatch between an SWG and a BWG with a constant curvature radius  $R_{\max}$  is evaluated according to the excitation ratios of the four TM modes in the BWG when any given TM mode is launched from the input SWG. The excitation ratios are obtained by calculating the overlap integral between the eigenmodes in the SWG and the eigenmodes in the BWG with a constant curvature radius  $R_{\max}$ . Here a Finite Difference Eigenmode (FDE) solver provided by Lumerical MODE Solutions is used. Figures 2(a)-2(d) show the calculated mode excitation ratio  $\xi_{ij}$  from the  $i$ -th TM mode launched at the input SWG to the  $j$ -th TM mode in the modified-Euler bend as the curvature radius  $R_{\max}$  varies for the cases with  $i = 0, 1, 2,$  and  $3,$  respectively. From the figures, one sees that the curvature radius  $R_{\max}$  should be  $>300 \mu\text{m}$  in order to make the undesired mode excitation ratio  $\xi_{ij}$  ( $i \neq j$ ) be less than  $-30 \text{ dB}$ . Here we choose  $R_{\max} = 600 \mu\text{m}$  to be safe considering the wavelength-dependence and fabrication errors. The minimum curvature radius  $R_{\min}$  is then determined according to the excess loss and inter-mode crosstalk calculated from the simulation of light propagation along a  $90^\circ$  modified Euler-bend as the radius  $R_{\min}$  varies. Here a three-dimensional (3D) finite-difference time domain (FDTD) method supported by Lumerical FDTD Solutions is used for simulating the light propagation in the whole structure consisting of an input SWG, a  $90^\circ$  modified Euler-bend, and an output SWG. We calculate the wavelength-dependence of the coupled power  $T_{ij}$  from the  $i$ -th TM mode at the input SWG to the  $j$ -th TM mode at the output SWG. Here the excess loss is given by  $\text{EL}_i = -10\log_{10}T_{ii}$  while the inter-mode crosstalk is given by  $\text{CT}_{ij} = 10\log_{10}T_{ij}$  ( $j \neq i$ ). Since the crosstalk between the  $\text{TM}_0$  mode and the  $\text{TM}_1$  mode is dominant, we focus on the case when the  $\text{TM}_0$  mode is launched. The calculated results for the coupled power  $T_{0j}$  with the cases of  $R_{\min} = 15, 20, 25,$  and  $30 \mu\text{m}$  are shown in Figs. 3(a)-3(d), respectively. From Figs. 3(a)-3(d), it can be seen that the inter-mode crosstalk  $\text{CT}_{ij}$  between the  $\text{TM}_0$  and  $\text{TM}_1$  modes is indeed the dominant one since the mode overlap between them is the largest among four modes when the mode profiles are distorted in the multimode waveguide bend. When choosing  $R_{\min} = 15 \mu\text{m}$ , the inter-mode crosstalk  $\text{CT}_{01}$  is as high as  $-10 \text{ dB}$  in the wavelength band of  $1500\sim 1600 \text{ nm}$ . It is not surprise that the crosstalk can be reduced by increasing the minimum curvature radius  $R_{\min}$ . For the present case, when increasing the minimum curvature radius to  $R_{\min} = 25 \mu\text{m}$ , the inter-mode crosstalk decreases to  $<-25 \text{ dB}$  and the excess loss is  $<0.04 \text{ dB}$ . In order to be compact, we choose  $R_{\min} = 25 \mu\text{m}$  in our case.

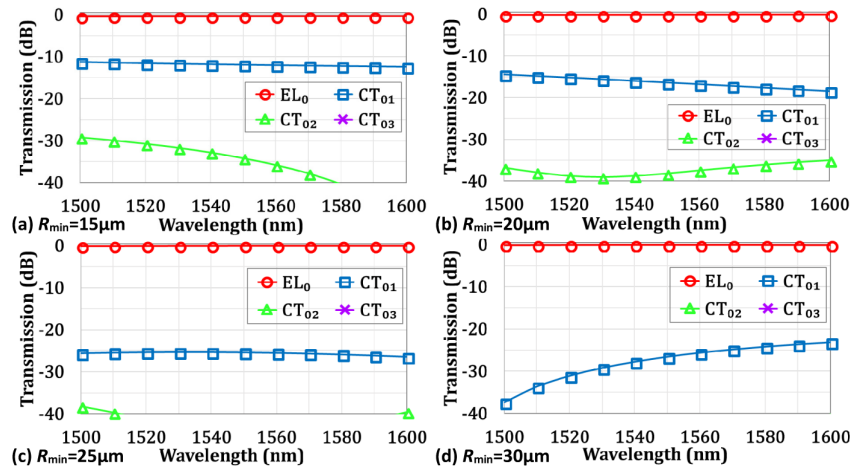


Fig. 3. Calculated transmissions in the whole structure consisting of an input SWG, a  $90^\circ$  modified Euler-bend, and an output SWG when the  $\text{TM}_0$  mode is launched at the input SWG. The  $90^\circ$  Euler bend is designed with  $R_{\min} = 15 \mu\text{m}$  (a),  $20 \mu\text{m}$  (b),  $25 \mu\text{m}$  (c), and  $30 \mu\text{m}$  (d). Here  $R_{\max} = 600 \mu\text{m}$ .

In the following parts, we set  $R_{\max} = 600 \mu\text{m}$  and  $R_{\min} = 25 \mu\text{m}$  for the modified  $90^\circ$  Euler-bend and simulate the light propagation in the multimode bus waveguide consisting of an input SWG, a  $90^\circ$  Euler-bend, and an output SWG. Figures 4(a)-4(d) show the calculated transmission  $T_{ij}$  from the  $i$ -th mode launched at the input SWG to the  $j$ -th mode in the output SWG for the cases with  $i = 0, 1, 2,$  and  $3,$  respectively. It can be seen that the excess losses are  $<0.04 \text{ dB}$  and the inter-mode crosstalk is  $<-25 \text{ dB}$  over a broad wavelength-band from  $1500 \text{ nm}$  to  $1600 \text{ nm}$  for all the 4 mode-channels. As a comparison, the transmissions  $T_{ij}$  for the cases with a  $90^\circ$  arc-bend are also calculated, as shown in Figs. 5(a)-5(d). In this case, the excess losses are  $\sim 1.5 \text{ dB}, \sim 1.5 \text{ dB}, \sim 0.3 \text{ dB},$  and  $\sim 0.3 \text{ dB}$  while the inter-mode crosstalks are as high as  $\sim -5 \text{ dB}, \sim -5 \text{ dB}, \sim -10 \text{ dB}, \sim -12 \text{ dB}$  for the  $\text{TM}_0, \text{TM}_1, \text{TM}_2,$  and  $\text{TM}_3$  modes, respectively. The present modified Euler-bend enables much lower excess losses and much lower inter-mode crosstalks than the regular arc-bend.

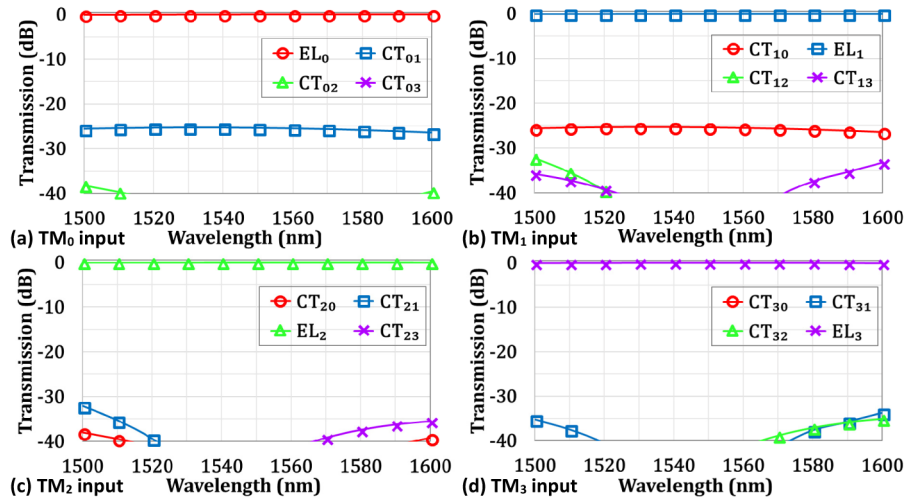


Fig. 4. Calculated transmissions  $T_{ij}$  from the  $i$ -th mode launched at the input SWG to the  $j$ -th TM mode in the output SWG for the cases with  $i = 0$  (a), 1 (b), 2 (c), and 3 (d), respectively. Here the modified  $90^\circ$  Euler-bend is with  $R_{\max} = 600 \mu\text{m}, R_{\min} = 25 \mu\text{m}$  and  $R_{\text{eff}} = 45 \mu\text{m}$ .

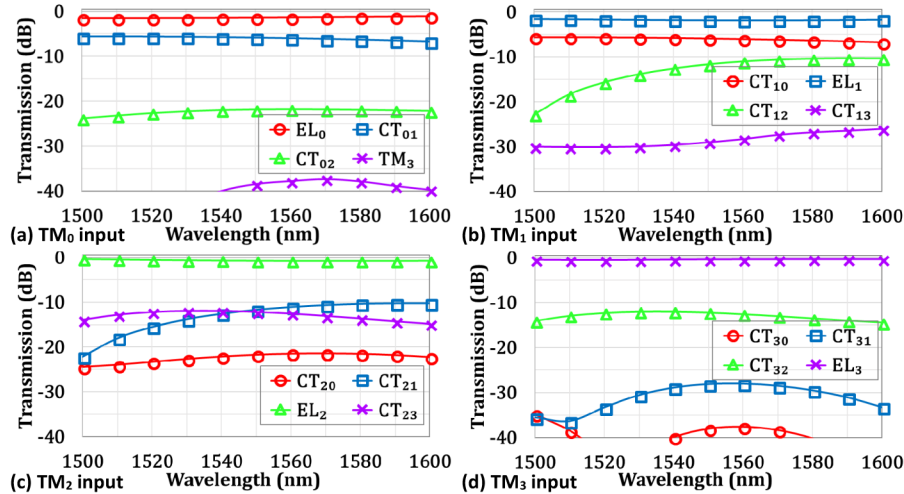


Fig. 5. Calculated transmissions  $T_{ij}$  from the  $i$ -th mode launched at the input SWG to the  $j$ -th TM mode in the output SWG for the cases with  $i = 0$  (a), 1 (b), 2 (c), and 3 (d), respectively. Here the  $90^\circ$  arc-bend is with  $R = 45 \mu\text{m}$ .

Figures 6(a)-6(d) show the simulated light propagation in the designed  $90^\circ$  Euler-bend with an effective radius  $R_{\text{eff}} = 45 \mu\text{m}$  (i.e.,  $R_{\text{max}} = 600 \mu\text{m}$ , and  $R_{\text{min}} = 25 \mu\text{m}$ ) when operating with  $\lambda_0 = 1550 \text{ nm}$  by launching different mode-channels ( $\text{TM}_i$ ) from the input SWG,  $i = 0, 1, 2,$  and  $3$ . The insets show the input/output mode field in the input/output SWGs. It can be seen that the electric field in the  $90^\circ$  Euler-bend is very uniform and no notable inter-mode crosstalks are observed. This verifies that the designed  $90^\circ$  Euler-bend indeed enables low-loss and low-crosstalk propagation for the launched  $\text{TM}_i$  mode. The light propagation in the regular  $90^\circ$  arc-bend is also simulated, as shown in Figs. 6(e)-6(h). Here the regular  $90^\circ$  arc-bend has a bending radius  $R = 45 \mu\text{m}$ , which is the same as the effective bending radius  $R_{\text{eff}}$  of the designed  $90^\circ$  Euler-bend. From Figs. 6(e)-6(h), notable multimode interference is observed when any mode-channel is launched from the input SWG. This indicates that more than one modes are excited in the  $90^\circ$  arc-bend and thus some significant undesired excess losses and crosstalks are introduced.

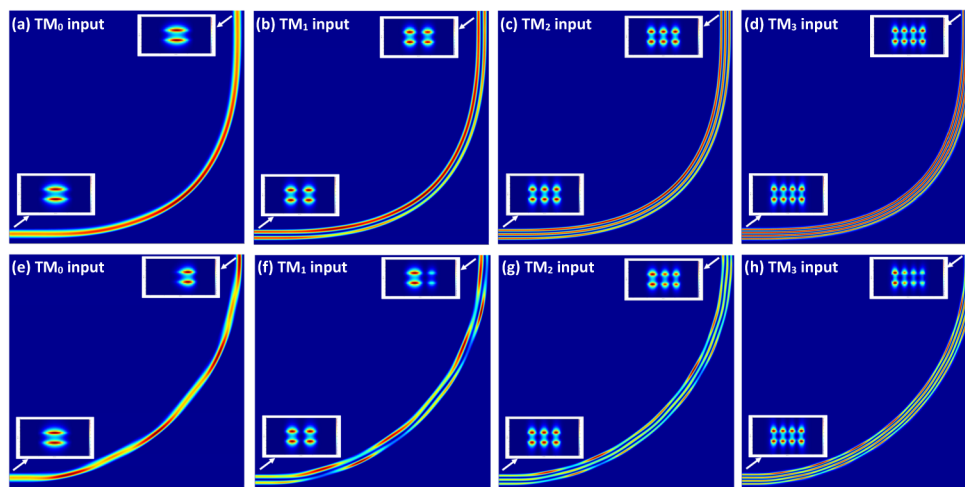


Fig. 6. Simulated light propagation in the designed  $90^\circ$  Euler-bend with  $R_{\text{eff}} = 45 \mu\text{m}$  (i.e.,  $R_{\text{max}} = 600 \mu\text{m}$ , and  $R_{\text{min}} = 25 \mu\text{m}$ ) (a-d) and the regular  $90^\circ$  arc-bend with  $R = 45 \mu\text{m}$  (e-h), when launching the  $\text{TM}_i$  mode-channel from the input SWG. Here  $i = 0$  (a, e), 1 (b, f), 2 (c, g), 3 (4, h).

### 3. Fabrication and measurement

The designed bent structures were fabricated on an SOI wafer with a 220 nm-thick top-silicon layer and a 2  $\mu\text{m}$ -thick buried-dioxide-layer. The processes of electron-beam lithography and ICP (inductively coupled plasma) dry-etching were applied to etch through the silicon core. The Microscope and scanning electron microscopic (SEM) images of the fabricated silicon PIC and the devices are shown in Fig. 7. The PIC consists of a 4-channel mode multiplexer ( $I_{\text{TM1}}, I_{\text{TM2}}, I_{\text{TM3}},$  and  $I_{\text{TM4}}$ ), a multimode bus waveguide with an S-bend, and a 4-channel mode demultiplexer ( $O_{\text{TM1}}, O_{\text{TM2}}, O_{\text{TM3}},$  and  $O_{\text{TM4}}$ ). The width of the multimode bus waveguide and the S-bend are 2.36  $\mu\text{m}$  as we designed in Sec. 2 for supporting four TM-polarization modes. Here the 4-channel mode (de)multiplexers are based on cascaded asymmetric directional couplers (ADCs) [25]. Focused grating couplers for TM-polarization were used for the chip-fiber coupling for the convenience of our lab. A broad-band amplified spontaneous emission (ASE) light source was used as the source and an optical spectrum analyzer was applied to readout the transmissions at the output ports. By launching light at each input port and monitoring the transmission at each output port, one can characterize the excess losses and inter-mode crosstalks for each mode-channel. The measured results were then normalized with respect to the transmission of a 450 nm-wide straight waveguide with grating couplers on the same chip.

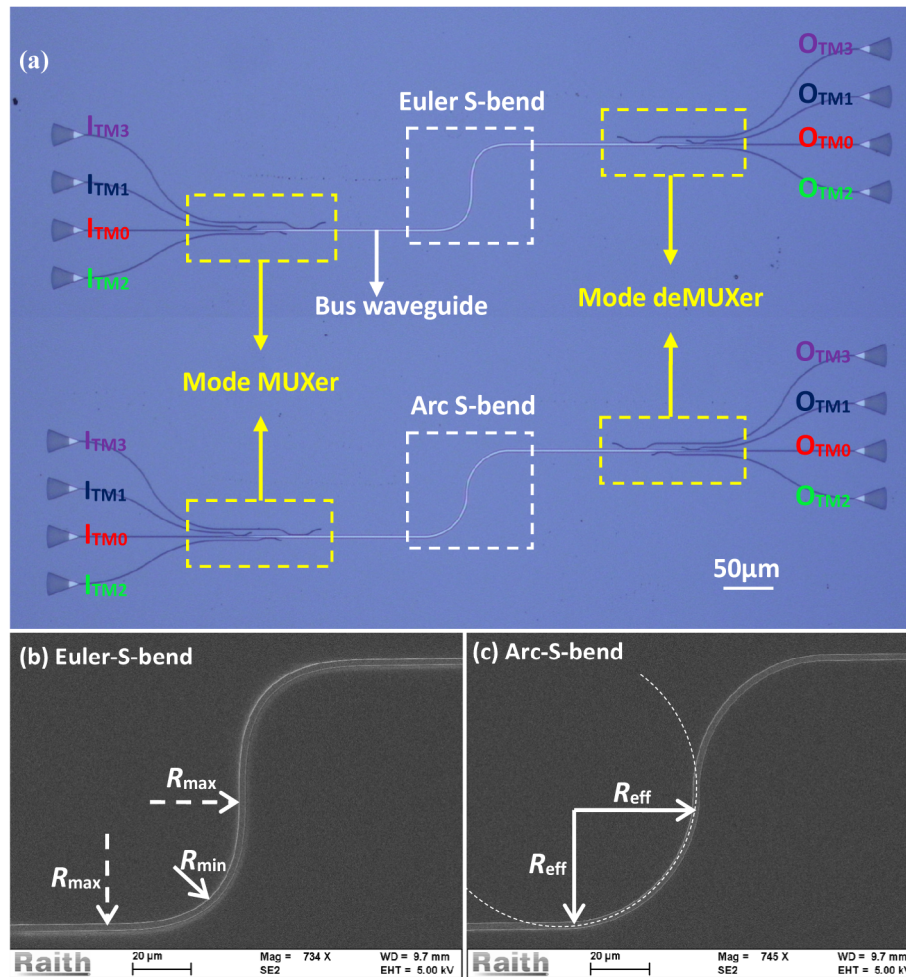


Fig. 7. Microscope image of the fabricated silicon PIC consists of a 4-channel mode multiplexer ( $I_{TM1}$ ,  $I_{TM2}$ ,  $I_{TM3}$ , and  $I_{TM4}$ ), a multimode bus waveguide with an S-bend, and 4-channel mode demultiplexer ( $O_{TM1}$ ,  $O_{TM2}$ ,  $O_{TM3}$ , and  $O_{TM4}$ ); (b) Scanning electron microscopic (SEM) images of the S-bends with two  $90^\circ$  Euler-bends; (c) SEM image of a  $90^\circ$  arc-bends.

Figures 8(a)-8(d) show the measured spectral responses of the transmissions for the fabricated silicon PIC consists of a 4-channel mode multiplexer, a fabricated S-bend with the  $90^\circ$  Euler-bends, and 4-channel mode demultiplexer. It can be seen that the inter-mode crosstalk is  $\sim -20$  dB over a broad band from 1520 nm to 1610 nm for all the four channels. To be specific, the measured crosstalk at the wavelength of 1550 nm is about  $-26.1$  dB,  $-21.4$  dB,  $-19.2$  dB, and  $-19.2$  dB for the  $TM_0$ ,  $TM_1$ ,  $TM_2$ , and  $TM_3$  modes, respectively. The crosstalks of the  $TM_0$  and  $TM_1$  are below  $-20$  dB over a 90 nm bandwidth. For the  $TM_2$  and  $TM_3$  modes, the crosstalk may rise to  $-18$  dB, as shown in Figs. 8(c)-(d). Some notable excess losses (2~5 dB) are also observed in the wavelength-band longer than 1580 nm for higher-order mode-channels. However, one should notice that the crosstalk level is apparently limited by the performance of the mode (de)multiplexers. Figures 9(a)-9(d) show the measured spectral responses of the transmissions for the silicon PIC consists of a 4-channel mode multiplexer, a straight multimode bus waveguide, and 4-channel mode demultiplexer when launching the  $TM_0$ ,  $TM_1$ ,  $TM_2$  and  $TM_3$  modes, respectively. When comparing with the measurement results shown in Figs. 8(a)-(d) and Figs. 9(a)-(d), it can be seen that the on-chip

mode (de)multiplexers are the dominant sources for the excess losses and the mode-channel crosstalks. For the on-chip mode (de)multiplexers, the excess losses are 0.2~5 dB and the inter-mode crosstalks are  $\sim$ -20 dB. This comparison shows that the present  $90^\circ$  Euler-bend has low excess losses of  $<0.5$  dB and low inter-mode crosstalks of  $<-20$  dB over a broad band from 1520 nm to 1610 nm for all the 4 mode-channels of TM polarization, which is consistent with the theoretical results given in Fig. 4. We also fabricated the PIC consisting an S-bend based on  $90^\circ$  arc-bends with  $R = 45 \mu\text{m}$  [see in Fig. 7(c)], and the measured spectral responses of the transmissions for all the 4 mode-channels are shown in Figs. 10(a)-(d). It can be seen that all four mode-channels have high excess losses, while the inter-mode crosstalks between  $\text{TM}_0$  and  $\text{TM}_1$ ,  $\text{TM}_2$  and  $\text{TM}_3$  are very large. This agrees well with the theoretical prediction shown in Figs. 5(a)-(d).

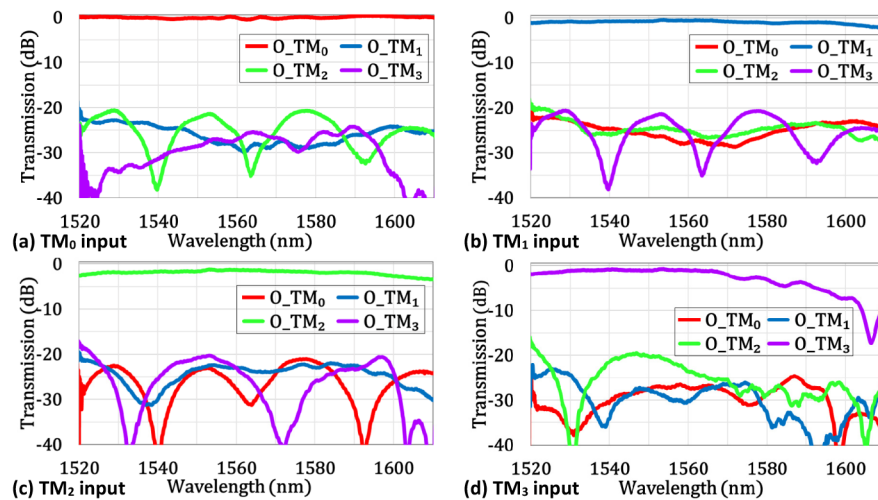


Fig. 8. Measured spectral responses of the transmissions for the fabricated silicon PIC consists of a 4-channel mode multiplexer, a fabricated S-bend with the  $90^\circ$  Euler-bends, and 4-channel mode demultiplexer when launching the  $\text{TM}_0$  (a),  $\text{TM}_1$  (b),  $\text{TM}_2$  (c) and  $\text{TM}_3$  (d) modes, respectively.

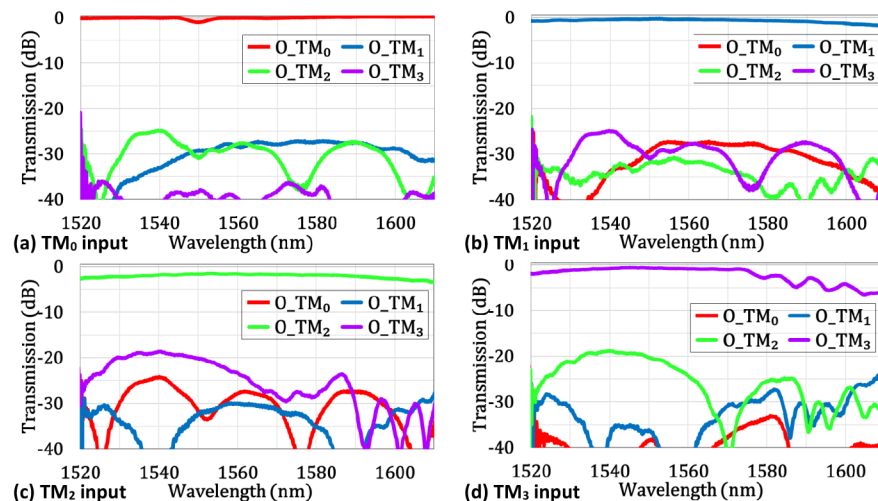


Fig. 9. Measured spectral responses of the transmissions for the silicon PIC consists of a 4-channel mode multiplexer, a straight multimode bus waveguide, and 4-channel mode demultiplexer when launching the  $\text{TM}_0$  (a),  $\text{TM}_1$  (b),  $\text{TM}_2$  (c) and  $\text{TM}_3$  (d) modes, respectively.

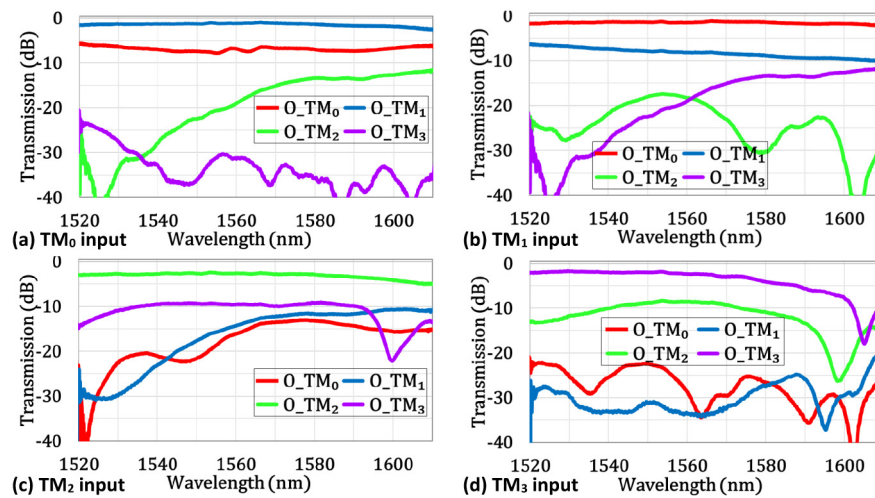


Fig. 10. Measured spectral responses of the transmissions for the PIC consists of a 4-channel mode multiplexer, a fabricated S-bend with the  $90^\circ$  arc-bends, and 4-channel mode demultiplexer when launching  $TM_0$  (a),  $TM_1$  (b),  $TM_2$  (c) and  $TM_3$  (d) modes, respectively.

#### 4. Conclusion

In summary, we have proposed and realized a low-loss and low-crosstalk multimode waveguide bend on silicon by introducing modified Euler-bends. In theory the designed  $90^\circ$  Euler-bend has very low excess losses ( $<0.1$  dB) and very low inter-mode crosstalk ( $<-25$  dB) with a compact effective radius as small as  $45 \mu\text{m}$ , which is about  $1/4$  of the radius ( $\sim 175 \mu\text{m}$ ) for a regular  $90^\circ$  arc-bend. Correspondingly, the occupied area is as small as  $1/16$  of that of the regular  $90^\circ$  arc-bend. For the present Euler-bend, there is no tiny structure and no additional fabrication steps are needed. Thus, the fabrication is easy and simple, including a one-step lithography and one-step dry-etching processes. Furthermore, the present Euler-bend insensitive to the variations of the core-width or the core-height in the bent section because of the adiabatic design. Silicon PICs consisting of a 4-channel mode multiplexer, a multimode bus waveguide with an S-bend consisting of two cascaded  $90^\circ$ -bends, a 4-channel mode demultiplexer have been designed and fabricated. The measurement results show that the fabricated Euler-S-bend has excess losses of  $<0.5$  dB and inter-mode crosstalks of  $<-20$  dB over a broad band from 1520 nm to 1610 nm for all 4 mode-channels of TM polarization. The present design can be extended for more mode-channels and also for TE-polarization when the multimode waveguide bend is designed carefully by optimizing the core-width and the bending radius. The proposed multimode waveguide bend is useful for on-chip MDM optical interconnects.

#### Funding

Zhejiang Provincial Natural Science Foundation (Z18F050002); National Natural Science Foundation of China (NSFC) (61725503, 61431166001, 11861121002); National Major Research and Development Program (No. 2016YFB0402502).